



Short communication

Synthesis and electrochemical properties of metals-doped LiFePO_4 prepared from the $\text{FeSO}_4 \cdot 7\text{H}_2\text{O}$ waste slag

Ling Wu, Xin-hai Li*, Zhi-xing Wang, Ling-jun Li, Jun-chao Zheng, Hua-jun Guo, Qi-yang Hu, Jie Fang

School of Metallurgical Science and Engineering, Central South University, Changsha 410083, China

ARTICLE INFO

Article history:

Received 22 July 2008

Received in revised form 23 August 2008

Accepted 28 August 2008

Available online 11 September 2008

Keywords:

Cathode material

LiFePO_4

$\text{FeSO}_4 \cdot 7\text{H}_2\text{O}$ waste slag

Doping

ABSTRACT

$\text{FePO}_4 \cdot x\text{H}_2\text{O}$ precursor was synthesized by using raw materials, $\text{FeSO}_4 \cdot 7\text{H}_2\text{O}$ waste slag and H_3PO_4 , without any purifying process. Crystalline metals-doped LiFePO_4 was prepared by heating an amorphous LiFePO_4 . The amorphous LiFePO_4 was obtained via a novel ambient temperature reduction method, using the as-prepared $\text{FePO}_4 \cdot x\text{H}_2\text{O}$, oxalic acid and Li_2CO_3 as raw materials. ICP analysis confirms that a small amount of Ti, Al and Ca deposited in precursor. XRD and Rietveld-refined results show that the metals-doped LiFePO_4 is single olivine-type phase and well crystallized, Ti atoms occupy Li (M1) site, resulting in the formation of cation-deficient solid solution. From SEM and corresponding elemental mapping images, it could be found that the particle size of LiFePO_4 is about 200–500 nm, and the distribution of elements (Fe, P and Ti) is homogeneous. The electrochemical performance of LiFePO_4 cathode was evaluated by galvanostatic charge/discharge test. The results indicate that the metals-doped LiFePO_4 , prepared from the $\text{FeSO}_4 \cdot 7\text{H}_2\text{O}$ waste slag, delivers a capacity of 161, 153, 145, 134 and 112 mAh g^{-1} at 0.1C, 0.5C, 1C, 2C and 5C rate, respectively, and shows an excellent cycling performance at moderate current rates (up to 2C).

© 2008 Elsevier B.V. All rights reserved.

1. Introduction

Titanium dioxide is widely used in the manufacture of paints, paper, varnishes, lacquer, printing inks, rubber, ceramics and food, etc. White titanium dioxide pigment is commercially manufactured by either a sulfate or chloride route. The sulfate route still produces about 50% of global production [1]. However, large quantity of $\text{FeSO}_4 \cdot 7\text{H}_2\text{O}$ waste slag is produced in the sulfate process, for example, to produce 1 ton pigment from ilmenite (containing TiO_2 , about 48%), about 3 tons $\text{FeSO}_4 \cdot 7\text{H}_2\text{O}$ waste slag would be produced [2]. In China, about 0.6 million tons of TiO_2 pigment is manufactured each year, of which more than 90% are operated with the sulfate route [3]. According to this, it can be estimated that about 1.62 million tons $\text{FeSO}_4 \cdot 7\text{H}_2\text{O}$ waste slag would be produced each year. Unfortunately, this waste slag is less marketable and hard to be utilized because of its high impurity contents, which causes not only severe environmental problems but also the waste of iron resource. Therefore, how to utilize the waste slag suitably has attracted great attention of the world.

Recently, some studies [4–6] have been focused on preparing magnetic ferric oxide from $\text{FeSO}_4 \cdot 7\text{H}_2\text{O}$ waste slag. However, these synthesis technics of preparing magnetic ferric oxide are complicated and consist of many purifying processes, due to the various impurities in the waste slag, such as Mg, Mn, Al, Ca, Ti, etc. Besides synthesis of magnetic ferric oxide, little work has been performed to utilize the $\text{FeSO}_4 \cdot 7\text{H}_2\text{O}$ waste slag. Hence, more simple and effective way to utilize the waste slag should be researched urgently.

In this study, a cathode material for lithium-ion batteries, metals-doped LiFePO_4 was prepared by using the $\text{FeSO}_4 \cdot 7\text{H}_2\text{O}$ waste slag (chemical composition is shown in Table 1) as raw material, and by a simple co-precipitation and ambient temperature reduction method. The whole route without any purifying process, owing to some impurities (Mg, Mn, Al, Ti, for example) benefit the electrochemical performance of LiFePO_4 [7–11]. It is noted that the metals-doped LiFePO_4 , prepared from the waste slag, exhibits excellent electrochemical properties.

2. Experimental

Metals-doped $\text{FePO}_4 \cdot x\text{H}_2\text{O}$ was synthesized by the following procedure: (1) $\text{FeSO}_4 \cdot 7\text{H}_2\text{O}$ waste slag (see Table 1) was dissolved in de-ionized water to obtain 0.25 M (Fe) solution, and the

* Corresponding author. Tel.: +86 731 8836633; fax: +86 731 8836633.
E-mail address: wuling19840404@163.com (L. Wu).

Table 1
Chemical composition (wt.%) of $\text{FeSO}_4 \cdot 7\text{H}_2\text{O}$ waste slag

$\text{FeSO}_4 \cdot 7\text{H}_2\text{O}$	88.52
$\text{MgSO}_4 \cdot 7\text{H}_2\text{O}$	6.04
$\text{MnSO}_4 \cdot 5\text{H}_2\text{O}$	0.35
$\text{Al}_2(\text{SO}_4)_3 \cdot 18\text{H}_2\text{O}$	0.28
$\text{CaSO}_4 \cdot 2\text{H}_2\text{O}$	0.18
TiOSO_4	0.52
Water insoluble	3.83
Others	0.28

solution was filtered to separate the water-insoluble; (2) H_3PO_4 (85 wt.%) was added to the solution, an equimolar solution of FeSO_4 and H_3PO_4 was obtained; (3) concentrated hydrogen peroxide (30 wt.%) was added to the solution under vigorous stirring; (4) then $\text{NH}_3 \cdot \text{H}_2\text{O}$ (2 M) was dropped into the solution to control the $\text{pH} = 2.1 \pm 0.1$, subsequently a white precipitate formed immediately; (5) after being stirred for 20 min, the precipitate was filtered, washed several times with de-ionized water and dried in an oven at 80°C . Thus, metals-doped $\text{FePO}_4 \cdot x\text{H}_2\text{O}$ powders were obtained.

Crystalline metals-doped LiFePO_4 was prepared by heating an amorphous LiFePO_4 in a tubular furnace at 600°C with flowing argon (99.999%) for 12 h. The amorphous LiFePO_4 obtained through lithiation of metals-doped $\text{FePO}_4 \cdot x\text{H}_2\text{O}$ by using oxalic acid as reducing agent at ambient temperature. Further experimental details can be found in Ref. [12].

The metals content of samples was analyzed using inductively coupled plasma emission spectroscopy (ICP, IRIS intrepid XSP, Thermo Electron Corporation), and the sulfur concentration by C–S analysis (Eltar, Germany). The SEM image and elemental mapping of the particles were observed with scanning electron microscopy (SEM, JEOL, JSM-5600LV). The powder X-ray diffraction (XRD, Rint-2000, Rigaku) using $\text{Cu K}\alpha$ radiation was employed to identify the crystalline phase of the synthesized material. X-ray Rietveld refinement was performed by FULLPROF.

The electrochemical performance was performed using a two-electrode coin-type cell (CR2025) of $\text{Li}|\text{LiPF}_6$ (EC:EMC:DMC = 1:1:1 in volume)| LiFePO_4 . The working cathode is composed of 80 wt.% LiFePO_4 powders, 10 wt.% acetylene black as conducting agent, and 10 wt.% poly(vinylidene fluoride) as binder. After being blended in *N*-methyl pyrrolidinone, the mixed slurry was spread uniformly on a thin aluminum foil and dried in vacuum for 12 h at 120°C . A metal lithium foil was used as anode. Electrodes were punched in the form of 14 mm diameter disks. A polypropylene micro-porous film was used as the separator. The assembly of the cells was carried out in a dry argon-filled glove box. The cells were charged and discharged over a voltage range of 2.5–4.1 V versus Li/Li^+ electrode at room temperature.

3. Results and discussion

The ICP results are given in Table 2. As shown, the molar ratio of Fe, Mg, Mn, Al, Ca and Ti, are 100:7.70:0.46:0.26:0.33:1.02 in raw material ($\text{FeSO}_4 \cdot 7\text{H}_2\text{O}$ waste slag), and 100:0:0:0.045:0.027:1.02 in product ($\text{FePO}_4 \cdot x\text{H}_2\text{O}$ precursor), respectively. The results demonstrate that 100% percentage of Ti, 17% percentage of Al and 8%

Table 2
The molar ratio of Fe, Mg, Mn, Al, Ca and Ti in raw material ($\text{FeSO}_4 \cdot 7\text{H}_2\text{O}$ waste slag) and product ($\text{FePO}_4 \cdot x\text{H}_2\text{O}$ precursor)

Samples	Fe	Mg	Mn	Al	Ca	Ti
$\text{FeSO}_4 \cdot 7\text{H}_2\text{O}$ waste slag	100	7.70	0.46	0.26	0.33	1.02
$\text{FePO}_4 \cdot x\text{H}_2\text{O}$ precursor	100	~0	~0	0.045	0.027	1.02

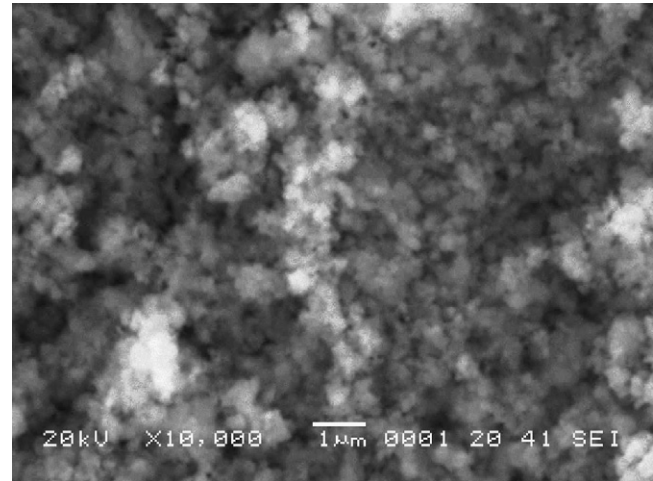


Fig. 1. SEM image of $\text{FePO}_4 \cdot x\text{H}_2\text{O}$ powders.

percentage of Ca were deposited in the precursor, however, Mg and Mn were not precipitated. As shown before, Ti and Al doping could improve the electrochemical performance of LiFePO_4 [7,8]. Ca doping, on the other hand, was seldom reported. In this paper, it is found that trace element Ca doped in LiFePO_4 did not affect its electrochemical properties obviously. Considering that sulfur residual content of precursor might impact the electrochemical performance of resulting LiFePO_4 , C–S analysis method was performed. The sulfur residual content of $\text{FePO}_4 \cdot x\text{H}_2\text{O}$ precursor is 0.80 wt.%, nevertheless, this content did not impact the electrochemical performance of resulting LiFePO_4 evidently, which will be proved in the following text.

The morphology of $\text{FePO}_4 \cdot x\text{H}_2\text{O}$ powders is shown in Fig. 1. $\text{FePO}_4 \cdot x\text{H}_2\text{O}$ sample exhibits a uniform fine-grained microstructure with particle size in the range of 100–200 nm. The nano-grade particles of precursor are conducive to the synthesis of LiFePO_4 fine powders.

Metals-doped LiFePO_4 was synthesized by the as-prepared precursor. Fig. 2 shows the Rietveld-refined X-ray diffraction pattern of metals-doped LiFePO_4 , and the crystal parameters are summarized in Table 3, the XRD pattern was refined without considering the trace elements (Al and Ca). As shown, the sample is single phase and well crystallized, all diffraction peaks are indexed in an orthorhombic system with the space group $Pnma$. The observed

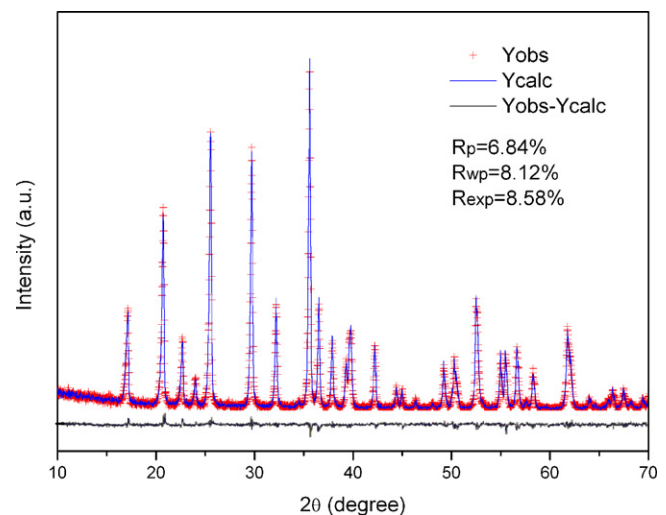


Fig. 2. The Rietveld-refined X-ray diffraction pattern of metals-doped LiFePO_4 .

Table 3
Results of structural analysis obtained from X-ray Rietveld refinement of metals-doped LiFePO₄

Atoms	Site	x	y	z	Occupancy	U_{iso} (Å ²)
Li	4a	0	0	0	0.958(4)	0.042(3)
Ti	4a	0	0	0	0.010(4)	0.040(5)
Fe	4c	0.2820(3)	0.25	0.9742(5)	1	0.030(8)
P	4c	0.0952(5)	0.25	0.4188(6)	1	0.026(2)
O1	4c	0.0961(6)	0.25	0.7420(2)	1	0.030(2)
O2	4c	0.4562(6)	0.25	0.2054(2)	1	0.024(3)
O3	8d	0.1648(8)	0.0484(8)	0.2835(4)	1	0.023(6)

Space group: *Pnma*. Cell constant (Å): $a = 10.3171(6)$, $b = 6.0009(4)$, $c = 4.6898(3)$; cell volume (Å³): 290.3598(4).

and calculated patterns match well, and the reliability factors are good ($R_p = 6.84\%$, $R_{wp} = 8.12\%$ and $R_{exp} = 8.58\%$). It is also indicated that the unit cell parameters $a = 10.3171(6)$ Å, $b = 6.0009(4)$ Å, and $c = 4.6898(3)$ Å obtained from the refinement are in good agreement with previously reported values [8]. In order to clarify whether Ti atoms occupy Li (M1) site or Fe (M2) site, the atom positions and occupancy were refined. Firstly, it is supposed Ti atoms occupy Fe site partially, however, the fitting result is bad and the reliability factors (R_p , R_{wp} and R_{exp}) are unacceptable. And then, it is assumed Ti atoms occupy Li site, as shown in Fig. 2, the fitting result is very good. This demonstrates that Ti atoms occupy Li (M1) site, and finally induce the formation of cation-deficient solid solution [7].

The primary particle size, d , was calculated from the X-ray line width using the Scherrer formula, $d = 0.9\lambda/\beta_{1/2} \cos \theta$, where λ is the X-ray wavelength, $\beta_{1/2}$ the corrected width of the main diffraction peak (1 3 1) at half height, and θ is the diffraction angle. The d value of the sample synthesized was found to be 41 nm. SEM image and EDS mapping (Fe, P and Ti) of LiFePO₄ are shown in Fig. 3. As shown, fine particles in the size of 200–500 nm can be observed. The particle size is much larger than the calculated value by the Scherrer formula, which should be attributed to particles aggregation. The distribution areas for elements (Fe, P and Ti) are homogeneous,

owing to the precipitation in the solution, which resulting in the atom-level mixed of different elements.

Fig. 4 shows the voltage profile with C-rate performances of metals-doped LiFePO₄ cathode in the voltage range of 2.5–4.1 V at room temperature. As shown, the initial discharge curve of LiFePO₄ shows a capacity of 161 mAh g⁻¹ at 0.1C rate (1C = 160 mA g⁻¹), which approaching the theoretical capacity of 170 mAh g⁻¹. By increasing the rate, the utilization percentage of the active material decreased, and 153, 145, 134 and 112 mAh g⁻¹ were delivered at 0.5C, 1C, 2C and 5C rates, respectively. From the shape of the charge and discharge profiles, LiFePO₄ electrode exhibited very long and flat plateau around 3.4 V even up to 2C rate, indicating little polarization. The excellent rate performance and small polarization of LiFePO₄ electrode should be ascribed to: (1) the metal elements doping, which intrinsically improve the bulk electronic conductivity of LiFePO₄ material by inducing an increased p-type semi-conductivity [7]; (2) the small particle size, which enhance the lithium ion diffusion speed [13].

Cycle stability of the metals-doped LiFePO₄ at room temperature is shown in Fig. 5. The cell cycled 10 times at 0.1C, then cycled 50 times at 0.5C, 1C, 2C and 5C in turn. The initial discharge capacity

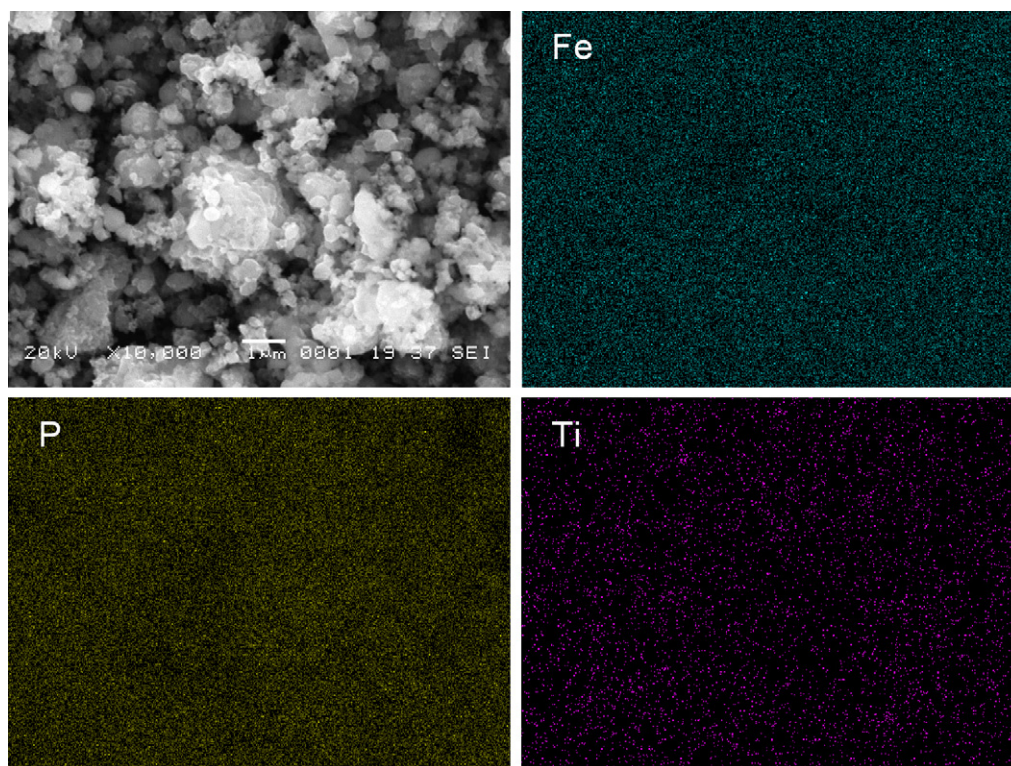


Fig. 3. SEM and EDS images of metals-doped LiFePO₄ synthesized at 600 °C, 12 h.

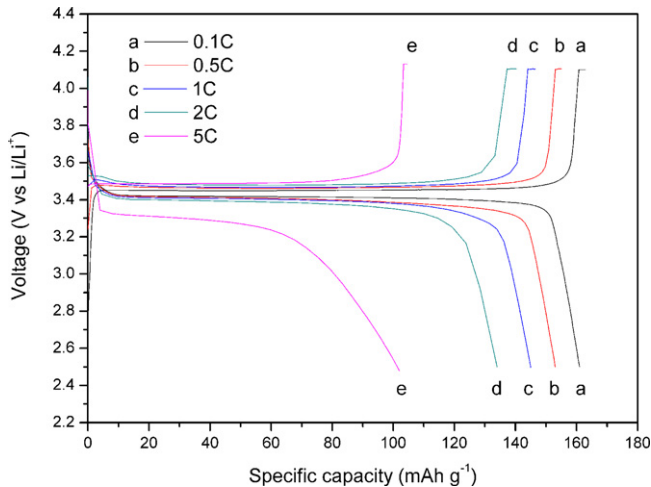


Fig. 4. The initial charge/discharge curves of metals-doped LiFePO₄ with different rates in the voltage range of 2.5–4.1 V at room temperature.

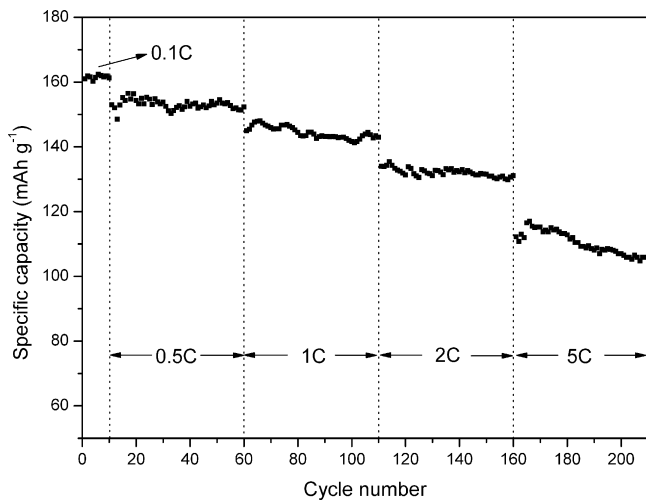


Fig. 5. Cycling performance of metals-doped LiFePO₄ at different rates. The cell cycled 10 times at 0.1C, then cycled 50 times at 0.5C, 1C, 2C and 5C in turn.

(mAh g⁻¹) of LiFePO₄ at the rate 0.5C, 1C, 2C and 5C is 153, 145, 134 and 112, respectively. Discharge capacities increased with cycles at first, and then waned with room temperature. After 50 cycles, the discharge capacity (mAh g⁻¹) at 0.5C, 1C, 2C and 5C is 152, 143, 131

and 106, and retains 99.3%, 98.6%, 97.8% and 94.6% of its initial discharge capacity, respectively. The metals-doped LiFePO₄ cathode shows an excellent cycling performance at moderate current rates (up to 2C), however, the cycle stability at high current rates (above 5C), still need to be improved.

4. Conclusion

FePO₄·xH₂O precursor was synthesized by using raw materials, FeSO₄·7H₂O waste slag and H₃PO₄, without any purifying process. ICP results show that 100% percentage of Ti, 17% percentage of Al and 8% percentage of Ca were deposited into the precursor, however, Mg and Mn were not precipitated. C–S analysis result shows that the sulfur residual content of precursor is 0.80 wt.%. Metals-doped LiFePO₄ was prepared by an ambient temperature reduction method, using the as-prepared precursor, oxalic acid and Li₂CO₃ as raw materials. The Rietveld-refined result of XRD pattern confirms that Ti atoms occupy Li (M1) site, resulting in the formation of cation-deficient solid solution. It is found that the sample, prepared from the FeSO₄·7H₂O waste slag, exhibits excellent electrochemical performance at moderate current rates (up to 2C), which demonstrates a very simple and feasible way to utilize the FeSO₄·7H₂O waste slag has been offered.

Acknowledgement

The project was sponsored by National Basic Research Program of China (973 Program, 2007CB613607).

References

- [1] B. Liang, C. Li, C. Zhang, Y. Zhang, *Hydrometallurgy* 76 (2005) 173.
- [2] M. Xu, M. Guo, J. Zhang, T. Wan, L. Kong, *J. Iron Steel Res. Int.* 13 (2006) 6.
- [3] C. Li, B. Liang, L. Guo, *Hydrometallurgy* 89 (2007) 1.
- [4] J.T. Nong, H. Huang, S.Q. Wei, *Chin. Patent* 200610018642.X (2007).
- [5] Z. Pang, R.H. Cai, Y.H. Lin, W.D. Tang, T.P. Chen, C.J. Xu, *Chin. Patent* 03150766.2 (2005).
- [6] S.N. Li, Q.M. Chen, C.X. Chen, C.H. Wang, X.J. Zou, *Chin. Patent* 00113589.9 (2004).
- [7] S.Y. Chung, J.T. Bloking, Y.M. Chiang, *Nat. Mater.* 1 (2002) 123.
- [8] G.X. Wang, S. Bewlay, S.A. Needham, H.K. Liu, R.S. Liu, V.A. Drozd, J.-F. Lee, J.M. Chen, *J. Electrochem. Soc.* 153 (2006) A25.
- [9] J. Molenda, W. Ojczyk, J. Marzec, *J. Power Sources* 174 (2007) 689.
- [10] D. Wang, H. Li, S. Shi, X. Huang, L. Chen, *Electrochim. Acta* 50 (2005) 2955.
- [11] T. Nakamura, K. Sakumoto, M. Okamoto, S. Seki, Y. Kobayashi, T. Takeuchi, M. Tabuchi, Y. Yamada, *J. Power Sources* 174 (2007) 435.
- [12] J.C. Zheng, X.H. Li, Z.X. Wang, H.J. Guo, S.Y. Zhou, *J. Power Sources* 184 (2008) 574.
- [13] A. Yamada, S.C. Chung, K. Hinokuma, *J. Electrochem. Soc.* 148 (2001) A224.